Friction and scratch resistance of polymer liquid crystals: Effects of magnetic field orientation

Witold Brostow[a)]
Laboratory of Advanced Polymers & Optimized Materials (LAPOM), Department of Materials Science and Engineering, College of Engineering, University of North Texas, Denton, Texas 76203-5310

Magdalena Jaklewicz
Department of Mechanical Engineering, McGill University, Montreal, Quebec, Canada H3A 2K6

(Received 16 July 2003; accepted 4 December 2003)

We have studied PET/0.6 PHB, an alternating copolymer in which PET is poly(ethylene terephthalate) and PHB is *p*-hydroxybenzoic acid with the mole fraction of 0.6 PHB. It is a longitudinal polymer liquid crystal (PLC) with the LC sequences in the main chain and oriented along the chain backbone. Material not subjected to the magnetic field, specimens oriented along and perpendicularly to the flux of the magnetic field, were investigated. Static friction, dynamic friction, scratch penetration depth, and healing of the material were determined. Static and dynamic friction parameters for oriented samples have significant higher values for oriented samples. The best scratch resistance is found for the sample aligned along the magnetic field. The results are explained in terms of morphology revealed by scanning electron microscopy and phase structures.

I. INTRODUCTION

A book reflecting extensively and well the contemporary status of polymer science and engineering in the world has been created by J.E. Mark.[1] In the subject index of his book, items such as tribology, wear, friction, and scratch resistance are absent. The same statement applies to the book by Goldman,[2] who discusses a variety of polymer deformation modes. On the other hand, Rabinowicz[3] has thoroughly covered the current status of tribology, and his book deals with metals almost exclusively. Thus, tribology is far better developed for metals than for polymers—though it represents in the latter case a rapidly expanding field of research.[4,5] Polymer tribology is difficult. For instance, contrary to expectations, in carbon-fiber–reinforced polymers the presence of fibers *lowers* the wear resistance of the neat polymers.[6] A chapter on polymers in a collective Swiss book on tribology[7] is largely limited to tabulated and diagramatically presented friction values. The need for understanding the tribological behavior of polymers is clear. In the first paper on polymer tribology from this group,[8] we have demonstrated that addition of a fluoropolymer to an epoxy before curing causes a significant lowering of both static and dynamic friction of the cured material. Then we have shown that the same additive increases the scratch resistance of the same commercial epoxy.[9] This time, we work on polymer liquid crystals (PLCs) because of their service extending to high temperatures, better mechanical properties than those of engineering polymers, low thermal expansivity, and other advantages.[10,11] In particular, we have studied orientation of PLCs in magnetic fields.[12,13] Though some work on tribology of liquid crystals (LC) state has been reported,[14,15] tribological properties strongly depend on the system in which a material functions.[16] In these circumstances, we have decided to investigate the effect of magnetic field orientation on static and dynamic friction, scratch resistance, and scratch healing of a PLC.

There are three key-variables one can play with while aligning the PLCs: the temperature of the experiment, the strength of the magnetic field applied, and the time of the exposition of sample to the field.

Selection of the orientation conditions for tribological testing is based on results of our earlier work.[12,13,17] The anisotropy increases significantly when one imposes a strong field and when the time of exposition is longer; due to viscoelastic inertia, the molecules react with some delay. Effects observed in Refs. 12 and 13 caused by temperature changes were explained on the basis of the phase diagram of PET/xPHB copolymers constructed before.[18] A rapid increase of anisotropy at temperatures above 250 °C has been found.[13]

[a)]Address all correspondence to this author.
e-mail: brostow@unt.edu
DOI: 10.1557/JMR.2004.0135

II. EXPERIMENTAL

A. Material

The material is the alternating copolymer of poly(ethylene terephthalate) (PET) + 0.6 mol fraction of *p*-hydroxybenzoic acid (PHB), denoted PET/0.6 PHB (sold under the trade name Rodrun-3000 by Unitica Corp., Osaka, Japan). It is a longitudinal thermotropic PLC that is with the rigid LC sequences in the main chain and oriented along the chain backbone.[11,17] This material has thoroughly been investigated and used by us earlier.[12,18–22] The PLC pellets were put through a high-speed thrashing machine and turned into a fibrous mass to avoid prealigning. The mass was kept at 100 °C for 5 h to remove any excess water and then in a dessicator before shaping into a variety of specimens. An oven was set to 250 °C, above the melting temperature of the PLC, T_m = 200 °C,[18] to facilitate the magnetic field alignment. A Teflon mold for the PLC bars was placed in an oven, and pressure was applied to ensure that there were no air bubbles trapped in the sample. No prealigned conditions detectable by x-ray method[12] were found. A miniature oven was placed in the small space between plates of the electromagnet. The sample was contained at a temperature defined during the set time for alignment, and the field was maintained after the set time. So as to preserve the alignment, the sample was then cooled below the lower glass transition temperature T_g of the two polymers constituting the copolymer, that is PET, for which T_g = 61 °C.[16] We have concluded[11] that appropriate conditions for good alignment of our material are 280 °C, 30 min exposure time, and 1.8 T. The selection of these values is based on our previous results. The orientation parameter defined in Ref. 12 reaches an approximately constant value in the temperature range 250–320 °C, hence 280 °C is in the middle of that range. At 280 °C, the orientation parameter reaches an asymptotic value after 25 min or so, hence 30 min exposition applied here. The 1.8 T field is relatively high to show significant effects and has been used before.[13]

Three different kinds of the PLC samples were prepared in the conditions just defined: nonoriented, henceforth labeled 0; aligned PLC with the longer axis of the sample parallel to the flux of the magnetic field $\vec{B}$ (sample II); and aligned PLC with the longer axis of the sample perpendicular to the flux of the magnetic field field $\vec{B}$ (sample L).

B. Friction

A SINTECH universal testing machine was used to determine the friction characteristics of our materials: a sled on which the parallelepipedic sample is attached and moving with respect to a stationary plane. The sample fixed on the back on the sled slides over the surface of the plane creating friction resistance. A load cell was used to measure the force needed to slide the sample over the plane. The tests were performed at the room temperature of 24 °C. A 44.6 N load cell and a sled with the nominal weight of 0.700 kg were used. The testing speed was 150 mm/min. A Teflon cospecimen was used. The results reported below are the averages each of 10 tests. The tests and the static and dynamic friction parameter calculations were carried out following the appropriate ASTM standard.[23]

C. Scratch resistance

A Micro-Scratch Tester (MST-CESEMEX) from CSEM Instruments (Neuchatel, Switzerland) was used to measure the scratch resistance. A diamond tip generates a controlled scratch on the surface of the sample. The indentor was of the Rockwell type made of diamond with the point radius of 200 μm. Each run included a prescan, the scan (scratch), and a postscan. The prescan served for the characterization of the topology of the sample before the scratch was made. The postscan was performed to measure the viscoelastic response of the material after the scratch was made (healing or recovery after a scratch). The topology of the surface was obtained before the scratch and after the scratch by applying the tip with a very small constant force (0.03 N). The accuracy of the depth determination was ±7.5 nm. A minimum of 15 scratches was performed for each sample under the constant load of 15 N; all numbers reported below are averages. The velocity of scratching was 5.3 mm/min, and the scan length was 3.00 mm. MST measures the load normal to the surface and the penetration depth. The apparatus is controlled from a personal computer; the software collects and displays the results using the CSEM Scratch Software, version 2.3.

III. FRICTIONAL PROPERTIES

First, control experiments were performed, with samples treated only thermally. No significant changes were observed. We assume that any changes discussed here are associated with imposition of the magnetic field. The dynamic and static parameters of friction for samples 0, II, and L (relative to sample 0) are presented in Fig. 1. The use of relative values is known to enhance the accuracy of the results. The standard error bars are marked. Shading (horizontal, vertical, and x-shaped) helps to distiguish the blocks.

Samples used for tribological studies were rectangular, with one axis longer by about 5 times than the other one. As expected, values of the ratio vary with the orientation of the materials. As clearly seen in Fig. 1, the ratio increases after aligning for both parameters, more so for dynamic friction. The ratio of the static friction parameters increase from 1 for the sample 0 (by definition) to 5.2 for the sample II and 2.8 for the sample L. At the

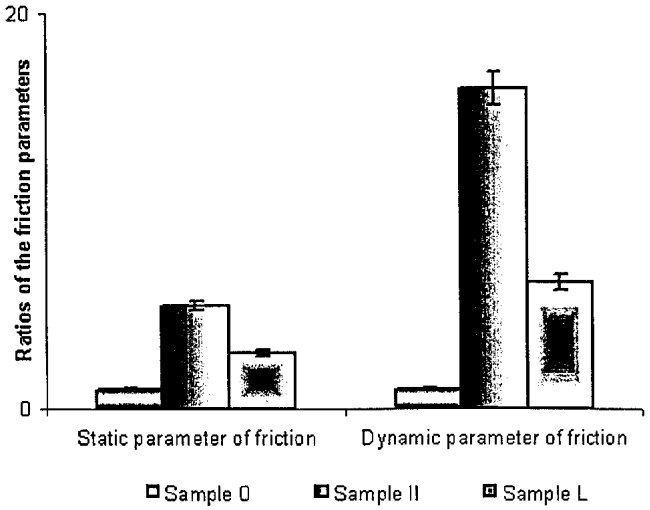

FIG. 1. The ratios of the static and the respective dynamic friction parameters measured for oriented samples II and L to the value measured for unoriented sample 0. The absolute values of the static and dynamic friction for sample 0 are 0.12 and 0.11, respectively, at the given test conditions.

same time, the ratios of the dynamic parameters increase from 1 for the sample 0 to 16.15 for the sample II and 6.4 for the sample L.

To explain the results seen in Fig. 1, consider the microphotographs of the PLC structure in Figs. 2 and 3. In Fig. 2 we see the two-phase material in the absence of the magnetic field. The LC-rich islands are small, more spherical than ellipsoidal. When the field is imposed, the growth of the islands reported in Refs. 10 and 11 is accompanied by their orientation and elongation along the field (Fig. 3). Rigid dispersoids make the material in the bulk harder and also change the character of the surface. One has to take also into account the sizes and spatial distribution of the islands.

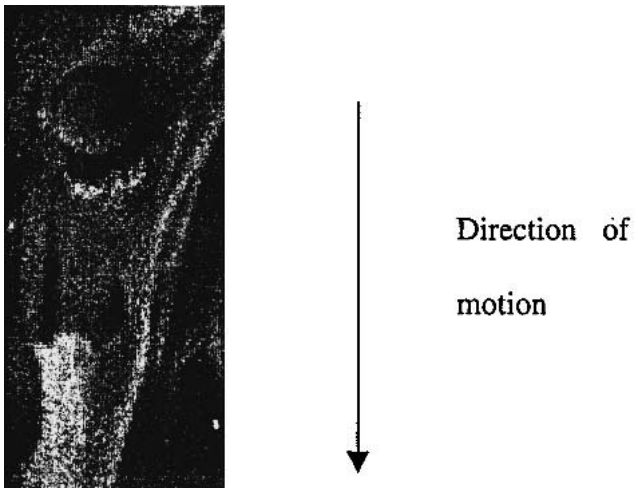

FIG. 2. SEM of the PLC material that has not been subjected to a magnetic field; one large LC island is visible. The image is recorded at the magnification of 10 k with a JEOL JSM–T300 Scanning Microscope; the sample was cooled with liquid nitrogen and immediately fractured, the fracture surface was coated with gold.

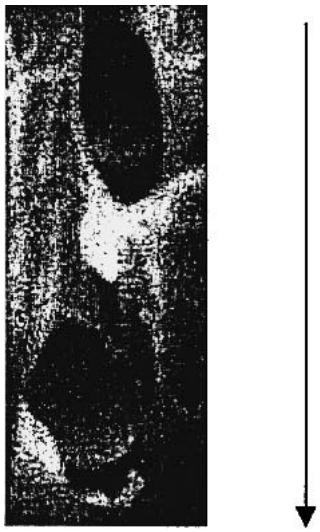

FIG. 3. A scanning electron micrograph of the PLC after imposition of the magnetic field (the conditions defined above in Sec. II); the image taken as described in the legend to Fig. 2. The vertical arrow defines the direction of field orientation. Comparison with Fig. 2 shows the growth and elongation of the islands caused by the field.

The islands in Fig. 3 are larger than in the sample in Fig. 2, which was not exposed to the field, hence more motion resistance is expected. Consider performing the experiment along the orientation direction (as the vertical arrow shows). During frictional motion parallel to the field, relatively large part of the sample trajectory goes over LC island surfaces. The islands offer more resistance to the movement than the LC-poor matrix, hence the high values of both static and dynamic friction for case II. In turn, go horizontally across Fig. 3, covering the same distance as before. The fraction of the movement trajectory that involves the islands is lower than in the case of sample II; however, it is still higher than in the unoriented sample seen in Fig. 2. It is for this reason that we see the intermediate values of static and dynamic friction in Fig. 1 for case L.

To explain why the relative dynamic friction for oriented sample is so much higher than the relative static friction, we need to consult the scanning electron microscopy (SEM) results of Hess and Lopez[24] for the same PLC. The beginning of the movement against surfaces such as shown in Fig. 9.5 in Ref. 24 along a feather or a bundle of fibers might be easier, before reaching the bundles border line. Thus, the feathery or fibrous surface seems to be responsible for dynamic friction values higher than respective static values.

IV. SCRATCH RESISTANCE

Typically, a viscoelastic material should recover or heal after the scratch. Comparison of the penetration

depth R_p and the residual depth R_h gives us the amount of healing ΔR

$$\Delta R = R_p - R_h \quad (1)$$

the surface has experienced after the scratch. In materials that heal well, necessarily the residual depth will be much less than the initial penetration depth. One expects that the amount of healing that takes place can be manipulated by the conditions of alignment—as we have done in this work.

In prescan, the profiles of the surfaces of the samples were taken and some irregularities noted. The profile values were used as the baseline. While the indentor was penetrating the materials, the scratch depth R_p was recorded.

We see in Fig. 4 that the penetration depth has a minimum value for the material oriented along the longer axis of the sample. The scratch resistance clearly increases after aligning. The penetration depth decreases in value from 258 μm for sample 0 to 178 μm for sample II and 199 μm for sample L. Thus, the value of the penetration depth for sample II is lower than the value for sample L. The explanation is somewhat similar to that for Fig. 1: longer parts of the trajectory covered by LC islands—which offer higher friction—also offer higher scratch resistance.

Viscoelastic recovery in oriented PLC is fast; after 3 min the bottom of the scratch stops moving. The recovery depth R_h values were recorded 5 min after the original scratch and then the ΔR values calculated from Eq. (1). The results are displayed in Fig. 5.

The healing manifests itself most for sample II, the respective value is 126.5 μm, and the least for sample 0, namely 60.2 μm; for sample L the value 77.5 μm is found.

Consult again Figs. 2 and 3. Smaller islands offer less resistance to the scratching diamond stylus. This is why the deepest penetration was obtained for microstructure presented in Fig. 2. At the same time, small LC-rich islands contribute little to the recovery capability–with the results seen in Fig. 5(a).

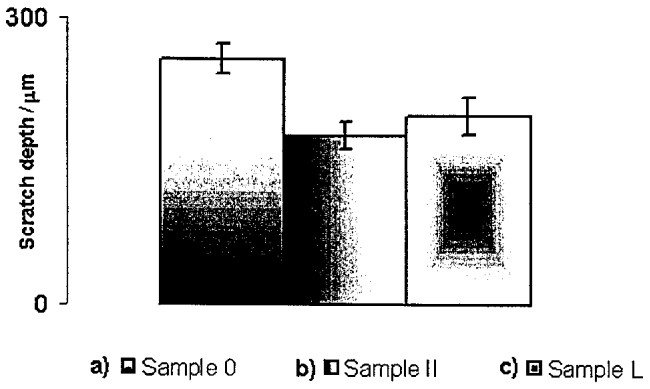

FIG. 4. Average of penetration depths during the scratch experiment.

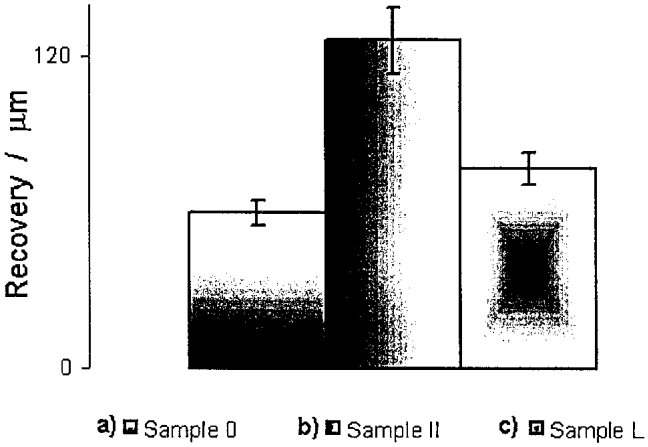

FIG. 5. Averages of the healing parameter ΔR in the PLC samples.

The second series to consider are Figs. 3 (followed in the vertical direction), 4(b), and 5(b). The diamond tip encounters the largest fraction of its path in the form of the LC islands. As already argued, this results in the lowest penetration depth in Fig. 4(b) and the highest recovery in Fig. 5(b). We recall results of molecular dynamic simulation of PLCs subjected to tensile forces:[25,26] cracks start and propagate until eventual fracture inside the flexible matrix rather than inside the islands. Although scratching differs from tension in the direction of force application to the material, we see that LC islands offer more resistance to both scratching and tension than the LC-poor matrix.

Behavior of the samples scratched perpendicularly to the orientation created by the magnetic field is seen in Figs. 4(c) and 5(c). Similarly as in the case of friction—and for analogous reasons—the behavior is intermediate between samples not subjected to the field and those in which the movement during tribological tests occurs perpendicularly to the longer axes of the islands. Thus, we see a common denominator between two classes of tribological properties, friction and scratch resistance. The movement direction with respect to the orientation of the minor phase and the fraction of the trajectory, which belongs to the minor (here strengthening) phase, determine frictional as well as scratching parameters.

V. DISCUSSION

Tribological properties have been determined for specimens placed in the magnetic field in two different directions. The results obtained for materials so aligned reveal interesting features. We clearly see that the alignment of the samples strongly affects the tribological properties of the PLC. The important aspect of the mechanism of altering the tribological properties of the

oriented PLC is the growth of the LC islands under the field imposition, studied earlier in terms of the microstructure.[10] We can treat the islands as dispersoids observed in alloys in several laboratories.[28–36] The islands are de facto dispersoids providing division of the surface into a soft phase (matrix) and a hard one (islands). We find that the dispersoids action is crucial also for the tribological properties of aligned PLC.

We note that much more work on polymer tribology is needed.[3,37,38] An 840 page book on polymer testing does not even have the word "wear" in its subject index[39] although surface wear is important in industry[40] as well as in medical applications of polymers.[41] The fact that in two-phase systems we have defined two factors that affect friction, scratch resistance and wear, is expected to be helpful.

ACKNOWLEDGMENTS

Partial financial support of this research has been provided by the State of Texas Advanced Research Program, Austin (Project No. 003594-0075-1999) and by the Robert A. Welch Foundation, Houston (Grant B-1203). Dr. Shreefal Mehta has participated in the magnetic field experiments. Mr. Tino Truong and Mr. Gwénaël Jegouic have participated in the friction and scratch data acquisitions. Dr. Anatoly Goldman of Alcoa CSI, Crawfordsville, Indiana, has provided useful comments on our work—as did three referees on our manuscript.

REFERENCES

1. *Physical Properties of Polymers Handbook*, edited by J.E. Mark (American Institute of Physics Press, Woodbury, NY, 1996).
2. A.Y. Goldman, *Prediction of Deformation Properties of Polymeric Composite Materials* (American Chemical Society, Washington, DC, 1994).
3. E. Rabinowicz, *Friction and Wear of Materials* (Wiley, New York, 1995).
4. S.W. Zhang, Tribol. Int. **31**, 49 (1998).
5. W. Brostow, J-L. Deborde, M. Jaklewicz, and P. Olszynski, J. Mater. Ed. **25,** (2003, in press).
6. *Friction and Wear Technology for Advanced Composite Materials*, edited by P.K. Rohatgi (ASM International, Materials Park, OH, 1994).
7. *Matériaux et contacts: une approche tribologique*, edited by G. Zambelli and L. Vincent (Presses Polytechniques Universitaires Romandes, Lausanne, 1998).
8. W. Brostow, P.E Cassidy, H.E. Hagg, M. Jaklewicz, and P.E. Montemartini, Polymer **42,** 7971 (2001).
9. W. Brostow, B. Bujard, P.E. Cassidy, H.E. Hagg, and P.E. Montemartini, Mater. Res. Innovat. **6,** 7 (2002).
10. W. Brostow, Polymer **31,** 979 (1990).
11. *Mechanical and Thermophysical Properties of Polymer Liquid Crystals*, edited by W. Brostow (Chapman & Hall, London, U.K., 1998).
12. W. Brostow, E.A. Faitelson, M.G. Kamensky, V.P. Korkhov, and Y.P. Rodin, Polymer **40,** 1441 (1999).
13. W. Brostow, M. Jaklewicz, S. Mehta, and P.E. Montemartini, Mater. Res. Innovat. **5,** 261 (2002).
14. *Tribology and the Liquid-Crystalline State*, edited by G. Biresaw (American Chemical Society, Washington, DC, 1990).
15. A.P. Harsha and U.S. Tewari, Polymer Testing **21,** 697 (2002).
16. H. Voss and K. Friedrich, Tribol. Int. **10,** 145 (1986).
17. W. Brostow, in *Physical Properties of Polymers Handbook*, edited by J.E. Mark (American Institute of Physics Press, Woodbury, NY, 1996), Ch. 33.
18. W. Brostow, M. Hess, and B.L. Lopez, Macromolecules **21,** 2262 (1994).
19. W. Brostow, B.L Lopez, and T. Sterzynski, Polymer **37,** 1551 (1996).
20. W. Brostow, B. Bujard, P.E. Cassidy, and S. Venumbaka, Polymer Int. **52,** 1498 (2003).
21. W. Brostow, T. Sterzynski, and S. Triouleyre, Polymer **37,** 1561 (1996).
22. W. Brostow, N.A. D'Souza, J. Kubat, and R. Maksimov, J. Chem. Phys. **110,** 9706 (1999).
23. ASTM D 1894–90, American Society for Testing and Materials, West Conshohocken, PA.
24. M. Hess and B.L. Lopez, in *Mechanical and Thermophysical Properties of Polymer Liquid Crystals*, edited by W. Brostow (Chapman & Hall, London, U.K., 1998).
25. W. Brostow, M. Donahue III, C.E. Karashin, and R. Simoes, Mater. Res. Innovat. **4,** 75 (2001).
26. W. Brostow, A.M. Cuhna, J. Quintanilla, and R. Simoes, Macromol. Theory Simul. **11,** 308 (2002).
27. W. Brostow, A.M. Cunha, and R. Simoes, Mater. Res. Innovat. **7,** 19 (2003).
28. A.K. Gupta and S.A. Lloyd, J. Mater. Sci. Eng. **301,** 140 (2001).
29. W.S. Sun and M.X. Quan, Mater. Lett. **27,** 101 (1996).
30. R. Behr, J. Mayer, and E. Arzt, Scr. Mater. **36,** 341 (1997).
31. L. Lu, M.O. Lai, and M.L. Hoe, Nanostructured Mater. **10,** 551 (1998).
32. E. Arzt, G. Dehm, P. Gumbsch, O. Kraft, and D. Weiss, Prog. Mater. Sci. **46,** 283 (2001).
33. S. Yang, A.M. Gokhale, and Z. Shan, Acta Mater. **48,** 2307 (2000).
34. M. Verelst, J.P. Bonino, and A. Rousset, Mater. Sci. Eng. A **135,** 51 (1991).
35. C.H. Caceres and J.R. Griffith, Acta Mater. **44,** 25 (1996).
36. T.A. Parthasarathy, M.G. Mendiratta, and D.M. Dimiduk, Scr. Mater. **37,** 315 (1997).
37. J. von Stebut, F. Lapostolle, M. Busca, and H. Vallen, Surf. Coat. Technol. **160,** 116 (1999).
38. G.H. Michler, *Kunststoff–Mikromechanik: Morphologie, Deformations–und Bruchmechanismen* (Hanser, München–Wien, 1992).
39. *Handbook of Polymer Testing*, edited by R. Brown (Marcel Dekker, New York–Basel, 1999).
40. F. Garbassi and E. Occhiello, in *Performance of Plastics*, edited by W. Brostow (Hanser, Cincinnati, OH, 2000), Ch. 16.
41. M. Deng and S.W. Shalaby, in *Performance of Plastics*, edited by W. Brostow (Hanser, Cincinnati, OH, 2000), Ch. 23.